AN APPRAISAL OF SOME SATELLITE RAINFALL PRODUCTS OVER AFRICA

Z. DEBO ADEYEWA[+]
Department of Meteorology, Federal University of Technology Akure, Nigeria.

(*Submitted*: 27 January 2005; *Accepted*: 19 July 2005)

Abstract
This paper presents the results of a three-year climatological appraisal of the rainfall products of the Tropical Rainfall Measuring Mission satellite Precipitation Radar (TRMM-PR), the Threshold-Matched Precipitation Index (TMPI) and the TRMM and Other Sources' (TRMM_OS) satellite data over Africa. Using the Global Precipitation Climatology Center (GPCC) rain gauge data at a grid resolution of 1.0 ° x 1.0 ° latitude/longitude, the study shows that generally, TRMM_OS has the best estimate. It has the lowest bias and root mean square error in all the seasons considered. The TRMM-PR has the highest bias and random errors. It has also been shown that the mean bias for all the algorithms for the whole continent is smallest in June-July-August (JJA). The paper appraises the systematic and random components of the error in the satellite algorithms. Analysis of the relative error showed that for each algorithm, reliability generally increased as the threshold rainfall increased. TRMM_OS has the lowest threshold and the highest reliability over Africa.

Keywords: Satellite rainfall products, validation, bias, random, systematic error.

1. Introduction

Africa, which is the second largest of the earth's seven continents, comprises 23 percent of the world's total land area. It has been estimated that some 13 percent of the world's population live in Africa (Microsoft Encarta Online Encyclopedia, 2001). In most parts of this vast continent, rain-fed agriculture is the method mostly practiced. Rainfall is therefore very crucial for the social and economic aspects of the numerous people on the continent. The reliability of rainfall data products for scientific, economic, and planning purposes is therefore very crucial.

Unfortunately, unlike in other major continents of the world, rain gauge measurement networks are very sparse and often irregular in Africa. Also, the Sahara, which occupies more than one-quarter of Africa, is the world's largest desert cutting a huge swath through the northern half of the continent with sparse rainfall and insufficient rainfall stations. Even in other regions such as the tropical rainforest areas, rainfall stations are not properly maintained and also sparsely distributed.

Thus, satellite observations of rainfall are the best solution for adequate temporal and spatial coverage of rainfall over Africa. Satellite-based precipitation products could provide very high temporal and spatial resolution (e.g. 3-hourly intervals on a 0.5°x0.5° latitude-longitude grid size). However, satellite derived rainfall products are subject to larger biases and stochastic errors; and need to be adjusted to in-situ observations (Barrett *et al*., 1994; Rudolf *et al*., 1996). Satellites have biases and random errors caused by factors such as the sampling frequency, the diurnal cycle of rainfall and the uncertainties in the rain retrieval algorithms (Bell *et al*., 1990; Kousky, 1980; Kummerow, 1998; Anagnostou *et al.*, 1999). Validations of satellite derived rainfall products are therefore essential to quantify the direct usability of these products.

For the land surface of the earth, rain gauge networks are still conventionally the most reliable source of area-averaged precipitation. It is generally known however, that although rain gauge observations produce relatively accurate point measurements of rainfall, they also suffer from sampling error in representing areal means. In addition, they are not available over most oceanic and unpopulated land areas (Xie and Arkin, 1996).

The Tropical Measuring Rainfall Mission (TRMM) Satellite was launched in 1997 with the sole objective of gaining a better understanding of precipitation structure and heating in the tropical regions of the earth (Simson *et al*., 1996). The TRMM satellite is operating on a non-sun synchronous orbit enabling it to observe tropical rainfall. It has a low altitude (350 km) and low inclination (35°). It completes one orbit around the earth in about 91 minutes, making it possible for it to cover the tropics with 16 orbits per day. The onboard instruments of TRMM include the Precipitation Radar (PR), Microwave Imager, Visible Infrared Scanner, Clouds and the Earth's Radiant Energy System and the Lightning Imaging Sensor. The most celebrated of these is the PR. This is because the TRMM-PR is the first space borne radar designed to capture more comprehensive structure of rainfall than any space-borne sensor before it. The TRMM-PR has been producing three-dimensional rainfall data from space unprecedented by any previous scientific spacecraft.

[+] formerly Adeyefa

Shin *et al.* (2001) have carried out a comparison of monthly rainfall derived from the TRMM TMI, PR, TRMM Combined Algorithm and the TMI-emission algorithm for two years (1998 and 1999). The results showed that for both the global and zonal means, the TMI rain rates were the largest while the PR estimates were the lowest. Also comparing the radar data from the TRMM satellite and Kwajalein Oceanic validation site, Schumacher and Houze (2000) observed that the temporal sampling of the TRMM radar accurately captured the Kwajelein radar's overall distribution of reflectivities and subdivisions into the different precipitation types. However, it was noted that the diurnal and the latitudinal variations of the precipitation in the vicinity were not well sampled. It could be noted that the 13.8 GHz frequency of TRMM-PR implies that the beam could be subject to attenuation in heavy precipitation areas such as the rainforest regions in Africa during the peak of the wet season. A first-order correction to such effects has been included in the algorithm (Iguchi *et al.,* 2000). The authors noted however, that the non-uniform rain distribution within the radar resolution cell might become a large source of error when the attenuation is severe.

The TRMM and Other Satellites/Sources (TRMM_OS) precipitation estimate is a combination of the TRMM Microwave Imager, the PR, and Visible-Infrared Scanner data with SSM/I, IR, and rain gauge data (Huffman *et al.*, 1995). Another satellite rainfall product used for the present study is the Threshold-Matched Precipitation Index (TMPI) satellite data available for latitude bands within 40°N - 40°S. More information on TRMM_OS and TMPI is provided in section 2.

In an earlier paper, Adeyewa and Nakamura (2003) focused mainly on regional characteristics of these precipitation products. It was shown that TRMM-PR has a large overestimation in the tropical rain forest region of Africa in December-January-February and in March-April-May. The bias is minimized in June-July-August and September-October-November. Generally, bias was shown to be high for all the satellite algorithms in the dry seasons when rainfall is minimal but it is less pronounced in the dry seasons of southern African climatic regions while TRMM_OS has the closest agreement with raingauge data. The paper showed that all the satellite algorithms exhibit significant seasonally and regionally dependent bias.

The present work provides a broad-scale outlook focusing on the African continent as a whole while providing further insight into the characteristics of the reliability of the rainfall products for the different climatic regions. The main objective of the paper is therefore to evaluate the TRMM-PR, TRMM_OS and TMPI data over the entire African region using the data for three years (36 months) for the various satellite algorithms.

2. Data Sources

The rain gauge data used for this study was obtained from the Global Precipitation Climatology Centre (GPCC) which is one of the major components of the Global Precipitation Climatology Project (GPCP) [Rudolf *et al.* (1994); Huffman *et al.* (1995); Huffman *et al*., (1997); Rudolf *et al*., (1998)]. The data is a global monthly precipitation for the land surface of the earth on a 1° x 1° latitude/longitude grid boxes. The total data used for Africa for each month is over 3000 grid points. Some rain gauge data obtained from some national meteorological establishments in Africa and the African Center of Meteorological Applications for Development (ACMAD) have been compared with that of GPCC and the results showed good agreement.

The TRMM PR standard monthly level 3 products (3A25) derived by the TRMM Science Team from level 2 instantaneous PR observations have been used for this study. The data covers tropical regions of the world within the 37°N to 37°S orbit of the TRMM satellite. The original 'fine grid' data at a resolution of 0.5° x 0.5° latitude/longitude grid cells have been re-gridded to 1.0° x 1.0° latitude/longitude cells to conform to the resolution obtainable from the other satellite products used in this study. The dataset archive consists of binary data sets in Hierarchical Data Format (HDF).

The Threshold-Matched Precipitation Index (TMPI) satellite data is part of the GPCP One-Degree Daily (1DD) precipitation product. The 1DD uses some "best" quasi-global observational estimators of underlying statistics to adjust quasi-global observational datasets that have desirable time/space coverage. The GPCP 1DD global precipitation dataset consists of TMPI data between 40°N - 40°S and the Adjusted TIROS Operational Vertical Sounder (ATOVS) dataset outside this band. It covers the latitudinal band within 40°N-S corresponding to the TMPI approximate instantaneous precipitation. It was produced from the geo-IR T_b with fill-in by re-scaled leo-IR GOES Precipitation Index (GPI). It was also produced from 3-hourly merged global infrared (IR) brightness temperature (T_b) histograms on a 1°x1° grid in the band 40°N-40°S. The TMPI product is based on satellite estimates of rainfall and rain gauge observations.

The TRMM and Other Sources' (TRMM_OS) precipitation estimate (Algorithm 3B43) is an operational product of the TRMM mission. This product, referred to, as "TRMM-best estimates" is a combination of the TRMM Microwave Imager, the PR, and Visible-Infrared Scanner data with SSM/I, IR, and rain gauge data. It is a combined observation-only dataset based on gauge measurements and satellite estimates of rainfall. The estimates are also in the HDF format and are on a calendar month temporal resolution at a 1°x1° latitude-longitude spatial resolution extending from 40 °N - 40 °S. The data coverage for the present study is three years (Dec. 1997-Nov. 2000) except for TRMM_OS for Dec. 1997 because its processing started in January 1998.

3. Methodology

The analyses presented here are based on 3-month averages: December-January-February (DJF), March-April-May (MAM), June-July-August (JJA) and September-October-November (SON) as well as on monthly basis. For the whole of Africa (20 °W-60 °E, 40 °N - 40 °S) and each algorithm, a 3-year Mean Bias Error (MBE, in mm) was evaluated as:

$$\mathrm{MBE} = \sum_{j=1}^{N} (\mathrm{Alg}_j - \mathrm{Ref}_j)/N \qquad (1)$$

where *Alg* refers to any of the three algorithms, TMPI, PR, or TRMM_OS and j, to a specific grid point. There are 6400 grid points altogether. Ref is the reference or observed value (GPCC rain gauge data or TRMM_OS) and N is the number of grid points with observations in the defined African region. The percentage or relative Mean Bias Error (%MBE) was estimated as

$$\mathrm{MBE}(\%) = \frac{\sum_{j=1}^{N} (\mathrm{Alg}_j - \mathrm{Ref}_j)/N}{\sum_{j=1}^{N} (\mathrm{Ref}_j)/N} \times 100 \qquad (2)$$

The %MBE is used to ascertain the systematic component of the error in an algorithm. The Root Mean Square Error (RMSE, in mm) was evaluated according to the conventional formula:

$$\sqrt{\frac{\sum_{j=1}^{N} (\mathrm{Alg}_j - \mathrm{Ref}_j)^2}{N}} \qquad (3)$$

The corresponding relative RMSE or %RMSE also used to appraise the random component of the algorithms is given as

$$\mathrm{RMSE}(\%) = \frac{\sqrt{\sum_{j=1}^{N} (\mathrm{Alg}_j - \mathrm{Ref}_j)^2/N}}{\sum_{j=1}^{N} (\mathrm{Ref}_j)/N} \times 100 \qquad (4)$$

The different components of the errors were estimated only when the mean data is available at a particular grid point for all the algorithms. The same number and location of grid points or observations have therefore been used for all the algorithms.

4. Results and Discussion

Figure 1 (6 panels) show sample scattergrams for the mean 3-year seasonal comparisons (DJF and JJA) between the GPCC rain gauge precipitation and those of GPCP-TMPI, TRMM_OS and TRMM-PR for the whole African continent. In general, TRMM_OS has the best correlation with rain gauge data. The correlation is generally high, ranging between 0.94 in JJA and 0.92 in the other seasons. The scattergrams for TRMM_OS for all the four seasons (MAM, and SON not shown) also reveal that its seasonal variation is minimal. On the other hand, TRMM-PR shows the largest scatter and indications of high overestimation for all the seasons of the year. The agreement of TRMM-PR with rain gauge data is highest in JJA with a coefficient of correlation of 0.69 and lowest in SON (0.59). In the intermediate range is TMPI. It has generally good agreement with rain gauge data with correlation coefficient ranging between 0.90 in DJF to 0.87 in SON. It is also seasonally more consistent than TRMM-PR. Both TRMM_OS and TMPI show some possibilities of underestimation for the mean rainfall in JJA generally higher than 300 mm. It is generally seen that the best correlations are obtained in JJA (northern summer) and the worst, in DJF (northern winter) and also during the transitional periods (MAM and SON). A similar analysis on monthly basis for the three years (not shown) reveals that the best agreement between PR and rain gauge data is in August and the worst in May and September. For TRMM_OS, the highest correlation (0.95) was also obtained in August but the lowest in December. With TMPI, the highest agreement was obtained in August (0.90) while the lowest (0.81) was also in the previous month (July). The low correlation in July for TMPI is due to the high scattering when rainfall exceeds a threshold value of 300 mm. For the whole continent therefore, the TRMM_OS exhibited the best agreement with rain gauge data.

With the better performance of TRMM_OS, similar analysis as above was conducted using the TRMM_OS as reference. To eliminate the bias that could emanate from the higher number of data points available for TRMM-PR, TMPI and TRMM_OS, the comparison was done for only grid points where rain gauge data is also available. The result (not shown) indicates a general improvement of TRMM-PR and TMPI performance. Using the correlation coefficient as an indicator of the agreement between the algorithms, the performance of TRMM-PR improved by 7 %, 13 %, 10 % and 13 % for DJF, MAM, JJA and SON respectively. For TMPI, the improvement is not as remarkable, varying between 7 % in DJF and 9 % in JJA. In MAM and SON, it is 8 %. The best agreement for TRMM-PR is still in JJA and the lowest in SON. The general overestimations of TRMM-PR is still glaring though slightly reduced.

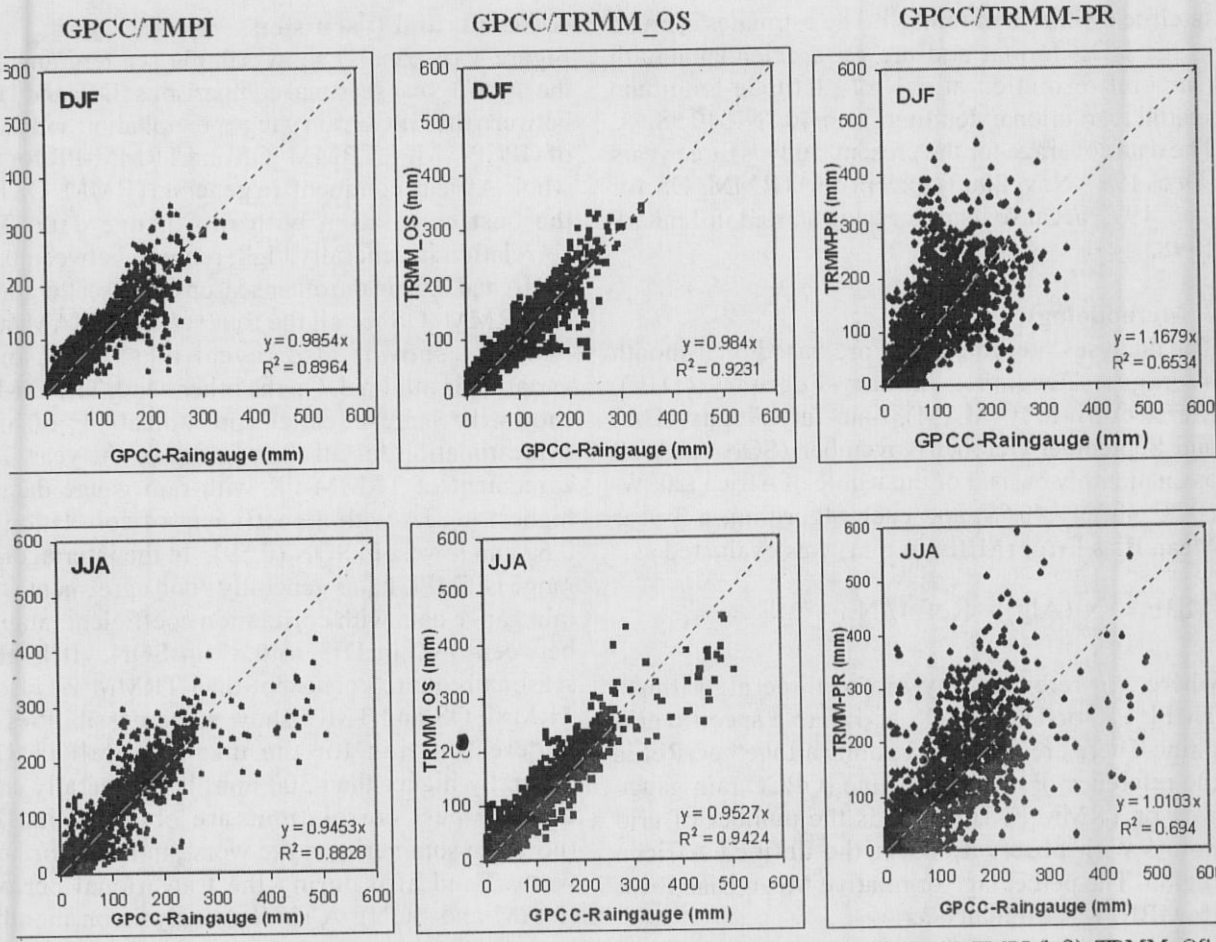

1a: Comparisons of mean seasonal (DJF and JJA) precipitation by GPCC rain gauge with GPCP-TMPI (left), TRMM_OS ddle) and TRMM-PR (right) for three years (Dec. 1997 – Nov. 2000) for the whole of Africa.

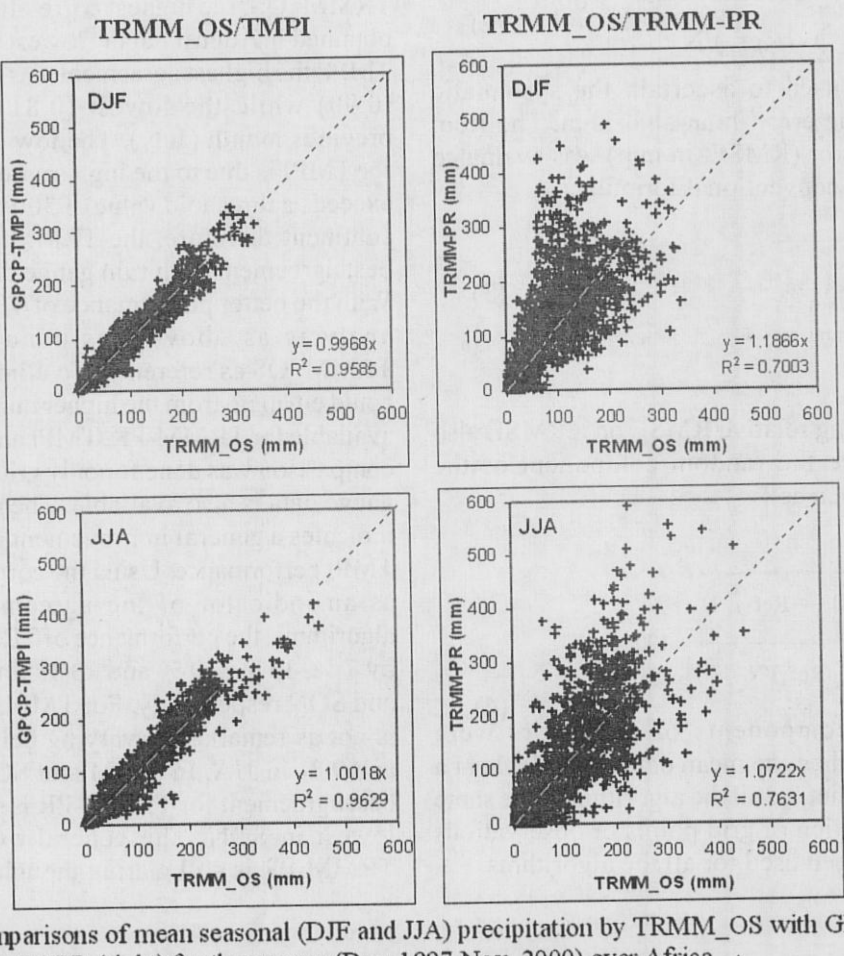

Fig. 1b: Comparisons of mean seasonal (DJF and JJA) precipitation by TRMM_OS with GPCP-TMPI (left) and TRMM-PR (right) for three years (Dec. 1997-Nov. 2000) over Africa.

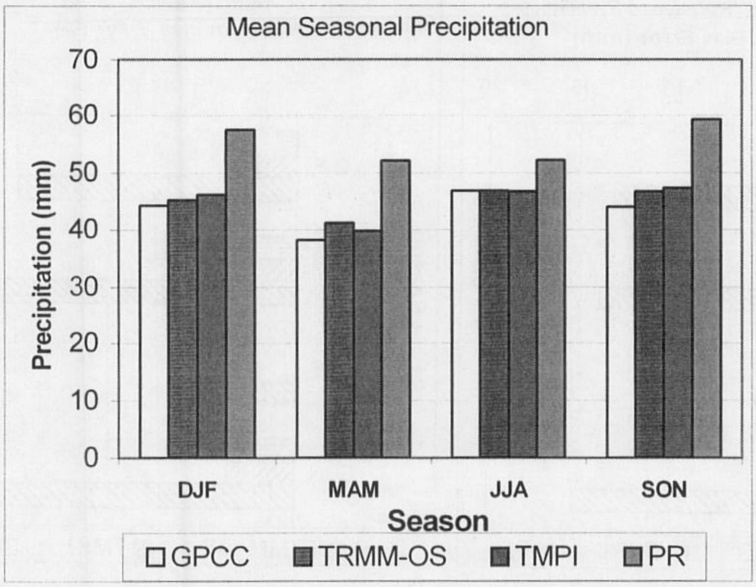

Fig. 2: Mean seasonal rainfall for entire Africa derived from GPCC rain gauge data, TRMM_OS, TMPI and TRMM-PR satellite estimates.

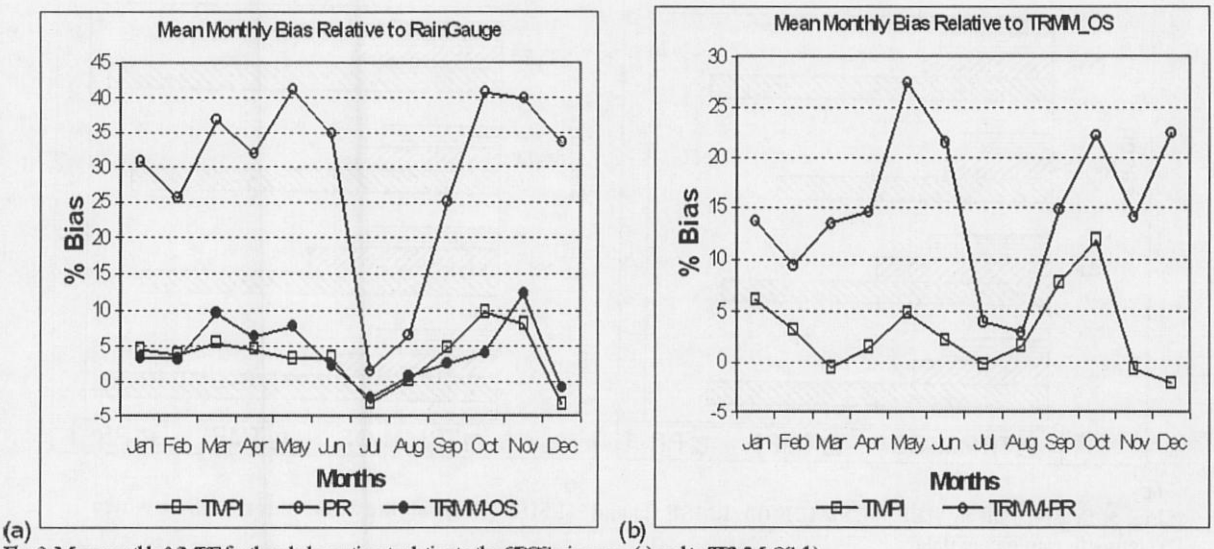

Fig. 3: Mean monthly %MBE for the whole continent relative to the GPCC rain gauge (a) and to TRMM_OS (b).

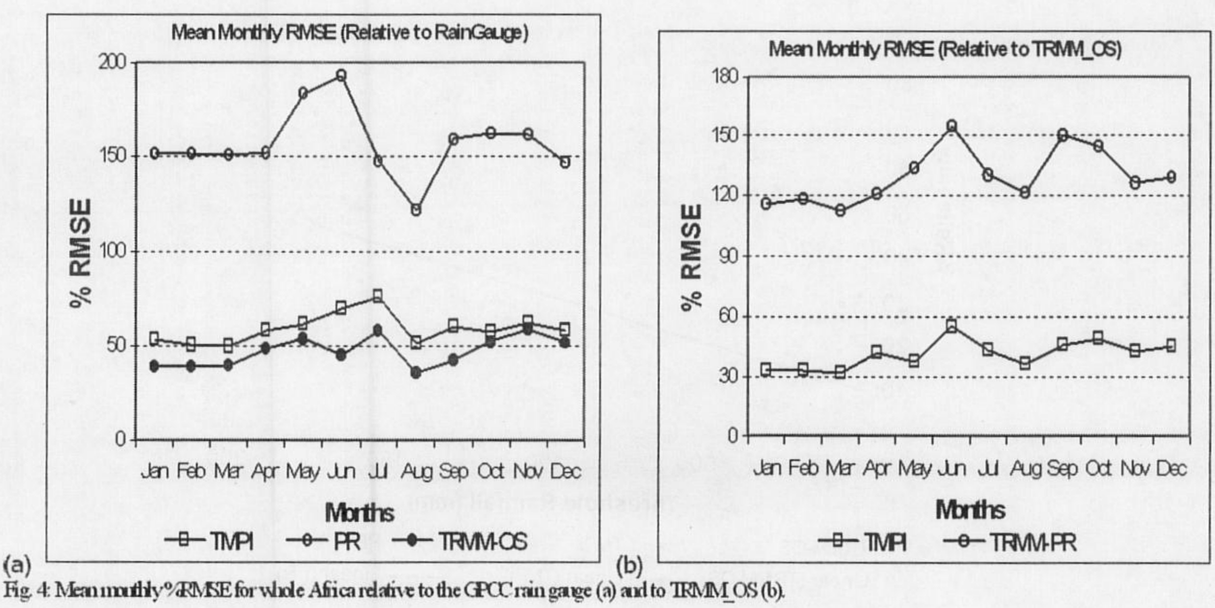

Fig. 4: Mean monthly %RMSE for whole Africa relative to the GPCC rain gauge (a) and to TRMM_OS (b).

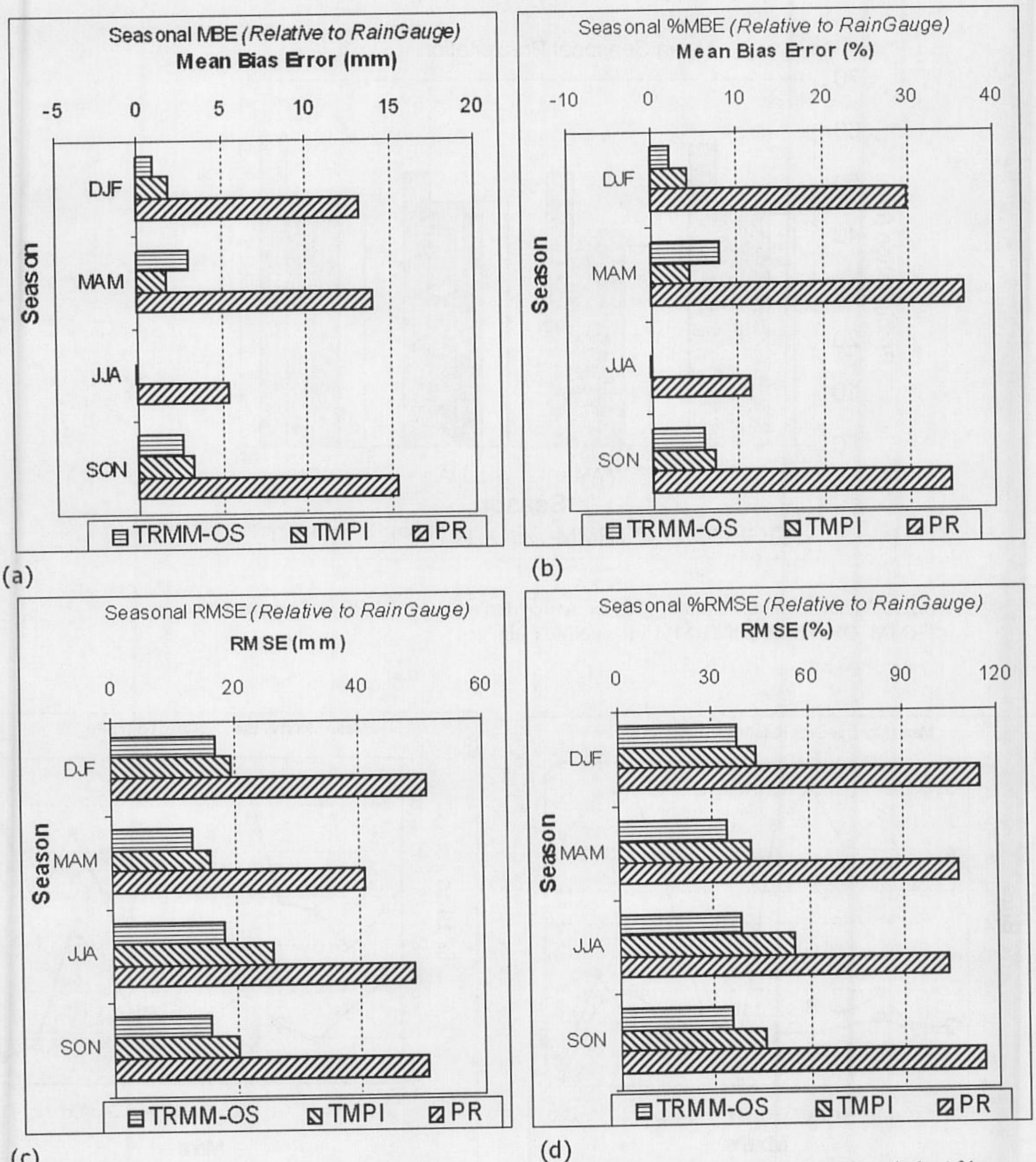

Fig. 5: Seasonal mean MBE (a), %MBE (b), RMSE (c) and %RMSE (d) for all the algorithms for whole Africa relative to rain gauge data.

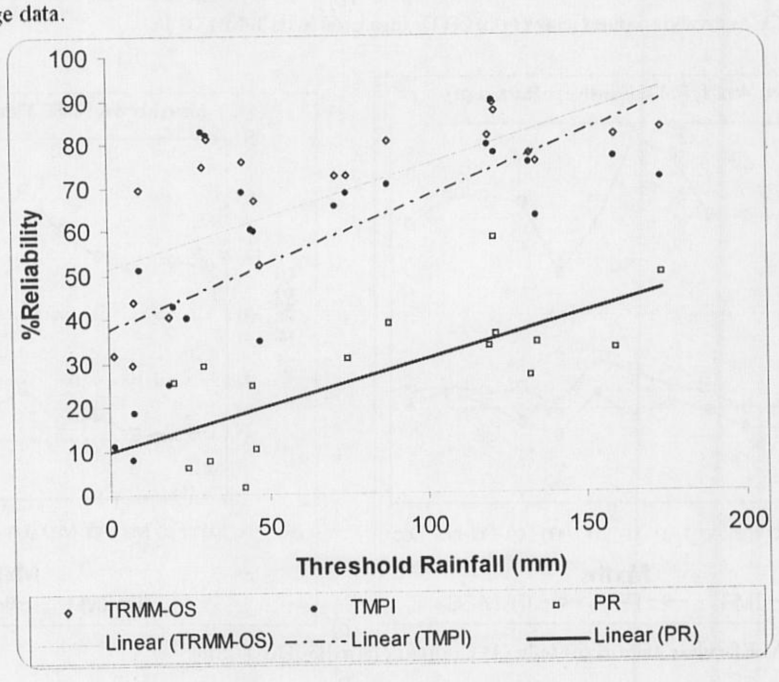

Fig. 6: Plot of reliability (%) as a function of threshold rainfall (mm).

The highest improvement of TRMM-PR in MAM and SON is noteworthy. One might treat this improvement as generally indicative of the unrepresentativeness in the rain gauge data during these transition periods.

Comparisons of mean seasonal rainfall for the entire Africa for the three satellite algorithms and GPCC rain gauge data are given in Fig. 2. GPCC estimates are close to those of TRMM_OS and TMPI. On the other hand, the overestimations of TRMM-PR are obvious in all the seasons. It is also seen that all the satellite algorithms tend to overestimate except in JJA for TRMM_OS and TMPI.

The mean monthly percentage biases (%MBE) for the whole continent relative to the GPCC rain gauge and to TRMM_OS are shown in Figs. 3a and 3b respectively. The biases were also estimated for all the algorithms only when rain gauge data is available. TRMM-PR generally overestimates with the bias ranging between 41 % in May/October and about 2 % in July. The bias is therefore lowest in the northern summer period but highest in May and October. The highest bias in May and October is due to the fact that these months correspond to transition periods in both northern and southern parts of Africa. Sampling error could therefore be high during the periods. For the other two algorithms, %MBE is much smaller varying only between -2 % (July) to +12 % (November) for TRMM_OS and between -3 % (December) and +10 % (October) for TMPI. It is rather notable that both TMPI and TRMM_OS generally underestimate in July while the bias of TRMM-PR is lowest at this period. Relative to TRMM_OS, TRMM-PR repeats a similar pattern but with lower bias (Fig. 3b). The highest bias (28 %) is still in May. In this regard, the bias of TMPI in October (12 %) is relatively higher than the earlier comparison with rain gauge.

As shown in Fig. 4a, the mean monthly RMSE of TRMM-PR relative to rain gauge data is quite high for the whole continent, exceeding 100 % for all the months of the year. The highest monthly RMSE (193 %) is in June and the lowest (122 %) in August. It hovers around 150 % in the other months. Noting that the relative bias in TRMM-PR is at the lowest in June, it implies that over all, the month of lowest systematic error also corresponds to the month of highest random error. For the TRMM_OS, the RMSE ranges between 36 % (August) and 59 % (Nov.) while for the TMPI, it is between 50% in Feb. and 76 % in July. The higher %RMSE in July for both could be interpreted as indicative of generally higher random error in this month. When the monthly %RMSE is computed with respect to TRMM_OS (Fig. 4b), the %RMSE for TRMM-PR and TMPI reduces generally by about 0-50 % for PR and 9-33 % for TMPI. June remains the month of highest random error.

On seasonal basis, the mean bias for all the algorithms for the whole continent is smallest in JJA. According to Fig. 5a, it is zero for TRMM_OS and negligible for TMPI but about 5 mm for TRMM-PR. This actually translates to a relative bias of 11 % for TRMM-PR and less than 0.5 % for TRMM_OS and TMPI (Fig. 5b). However, the RMSE for this period is not the lowest. It is almost 50 mm (104 %) for TRMM-PR and 18 mm (39 %) for TRMM_OS and 26 mm (56 %) for TMPI (Figs. 5c and 5d). For TRMM-PR and TMPI, bias is highest in SON with a correspondingly high RMSE (50 % and 21 % respectively). In all the seasons, the bias of the TRMM_OS is the lowest, generally within 0 - 3 mm (0-8 %) and RMSE of 13-18 mm (34-39 %). It is noteworthy that although the RMSE for TRMM-PR is lowest in MAM (41 mm), for a mean precipitation of 38 mm per month during this period, the %RMSE is still relatively high (115%). With TRMM_OS as reference, the mean bias for TRMM-PR and TMPI decreases respectively, by 0 % (JJA) to 10 % (MAM) and 0 % (JJA) to 8 % (MAM). In terms of %RMSE, the decrease for TRMM-PR is also highest in MAM (18 %) and lowest in DJF (9 %). However, the decrease is highest for TMPI in JJA (25 %).

An index of reliability for each region was obtained by using the inverse of the relative standard error of each algorithm for the four seasons under consideration. The characteristics of the climatic regions used are presented in Table 1 while the summary of the reliability of the precipitation data of the algorithms is given in Table 2. The seasons (3-month periods) for which the relative standard error of each algorithm is less than 100 % in each climatic region is referred to as applicable seasons. The threshold or observed minimum seasonal mean rainfall is also indicated. The table shows that for TRMM-PR, the precipitation data is not reliable in any season in the north African arid region since the inherent error in its estimation generally exceeds the actual or reference rainfall amount. In the northern semi-arid region, TRMM-PR rainfall data is only reliable in two seasons (JJA and SON). Its reliability increases in the wetter regions and seasons of the tropical-wet and the northern and southern savanna regions and also in the southern semi-arid. The lowest threshold of TRMM-PR (21 mm/month) is over the south Atlantic Ocean. On the other hand, the precipitation data of the TMPI and TRMM_OS are reliable in most of the climatic regions and the threshold rainfall is also quite low. The only exceptions to this are in the dry seasons of the northern regions.

As shown in Fig. 6, for each algorithm, reliability generally increased as the threshold rainfall increased, implying that higher rainfall amount than those shown in Table 1 would provide better reliability. TRMM_OS has the highest reliability and therefore, the lowest threshold in each region. The difference is significant at lower mean seasonal rainfall. At lower threshold, TRMM_OS is at least, 10 % more reliable than TMPI and 40 % than TRMM-PR in the climatic regions.

5. Summary and Conclusions

A 36-month climatological assessment of the TRMM-PR, TRMM_OS and GPCP-TMPI satellite products has been conducted at a grid resolution of 1.0°x1.0° latitude/longitude over Africa. The study shows that generally, TRMM_OS has the best agreement with rain gauge data. Generally, TRMM_OS has the lowest bias and random error in all the seasons considered. The GPCP-TMPI algorithm has been shown to perform better than the TRMM-PR. It has also been shown that the mean bias (mm) for all the algorithms for the whole continent is smallest in JJA, being negligible for TMPI and TRMM_OS but up to 11 % for TRMM-PR. For the whole African region, June corresponds to the month of lowest systematic error for TRMM-PR but also the month of highest random error for the algorithm. The high systematic error of TRMM-PR over Africa could be due to sampling error which results from the fact that only snapshots of the precipitation field is measured. This mainly results from the orbit characteristics of the TRMM satellite. It is obvious from these analyses, that the TRMM_OS rainfall product is more reliable over the African continent. Of the three satellite algorithms considered, only the TRMM-PR is a single-sourced satellite algorithm. As mentioned earlier, the TRMM_OS and TMPI precipitation estimates are based on the combination of multiple satellite and rain gauge data sets. The better performance of the two algorithms is therefore understandable although a better performance was expected from the TRMM-PR. In spite of its overestimation over Africa, the TRMM-PR data is still unique in terms of its regular provisions of 3-dimensional rainfall and storm structure information over Africa, more so as the continent is very deficient in radar coverage.

REFERENCES

Adeyewa, Z.D. and Nakamura, K., 2003. Validation of TRMM Radar Rainfall Data over Major Climatic Regions in Africa. *Journal of Applied Meteorology*, Vol. 42, No. 2, pp. 331-347.

Anagnostou, E.N., Emmanouil, N., Andrew, J., Negri, Robert, F., Adler, 1999. Statistical Adjustment of Satellite Microwave Monthly Rainfall Estimates over Amazonia. *J. of Appl. Meteor.*, 38(11), 1590-1598.

Barrett, E.C., Doodge, J., Goodman, M., Janowiak, J., Smith, E. and Kidd, C., 1994. The First WetNet Precipitation Intercomparison Project (PIP-1). *Remote Sensing Review*, 11(1-4), 49-60.

Bell, T.L., Abdullah, A., Martin, R.L. and North, G.R., 1990. Sampling Errors for Satellite-derived Tropical Rainfall: Monte Carlo Study Using Space-time stochastic model. *J. Geophys. Res.* 95, 2195-2206.

Huffman, G.J., Adler, R.F., Rudolf, B., Schneider, U. and Keehn, P.R., 1995. Global Precipitation Estimates Based on a Technique for Combining Satellite-Based Estimates, Raingauge Analyses and NWP Model Information. *J. Climate,* 8(5), 1284-1295.

Huffman, G.J., Adler, R.F., Arkin, P.A., Chang, A., Ferraro, R., Gruber, A., Janowiak, J., McNab, A., Rudolf, B. and Schneider, U., 1997. The Global Precipitation Climatology Project (GPCP) Combined Precipitation Dataset. *Bull. Amer. Meteor. Soc.*, 78(1), 5-20.

Iguchi, Toshio, Toshiaki Kozu, Robert Meneghini, Jun Awaka, Ken'ichi Okamoto, 2000. Rain-Profiling Algorithm for the TRMM Precipitation Radar. *J. of Appl. Meteor.,* 39(12) 2038–2052.

Kousky, V.E., 1980. Diurnal Rainfall variation in Northeast Brazil. *Mon. Wea. Rev.*, 108, 488-498

Kummerow, C., 1998. Beamfilling Errors in Passive Microwave Rainfall Retrievals. *J. of Appl. Meteor.*, 37, 356-357.

Microsoft Encarta Online Encyclopedia, 2001. Africa. http://encarta.msn.com. Microsoft Corporation.

Rudolf, B., Hauschild, H., Rueth, W. and Schneider, U., 1994. Terrestrial Precipitation Analysis: Operational Method and Required Density of Point Measurements. NATO ASI I/26, *Global Precipitations and Climate Change,* M. Desbois and F. Desalmand (Eds.), Springer Verlag Berlin, 173-186.

Rudolf, B., Hauschild, H., Rueth, W. and Schneider, U., 1996. Comparison of Raingauge Analyses, Satellite-Based Precipitation Estimates and Forecast Model Results. *Advances in Space Research*, 18(7), 53-62.

Rudolf, B., Fuchs, T., Rueth, W. and Schneider, U., 1998. Precipitation Data for Verification of NWP Model Re-Analyses: The Accuracy of Observational Results. Proceedings WCRP International Conference on Reanalyses, Washington, DC, 27-31 Oct. 1997, *WCRP* 104, WMO/TD-No. 876, 215-218.

Schumacher, Courtney, Robert, A., Houze, Jr., 2000. Comparison of Radar Data from the TRMM Satellite and Kwajalein Oceanic Validation Site. *J. of Appl. Meteor.*: 39(12) 2151-2164.

Shin, Dong-Bin, Long, S., Chiu, and Menas Kafatos, 2001. Comparison of Monthly Precipitation Derived from the TRMM Satellite. *Geophysical Research Letters*. 28(5), 795-798.

Simson, J., Kummerow, C., Tao, W.K. and Adler, R.F., 1996. On the Tropical Rainfall Measuring Mission (TRMM). *Meteor. Atmos. Phys.*, 60, 19-36.

Xie, Pingping and Arkin, P.A., 1996. Analyses of Global Monthly Precipitation Using Gauge Observations, Satellite Estimates, and Numerical Model Predictions. *J. Climate*: 9(4), 840-858.

Table 1: Major climatic regions of Africa used for the study.

Climatic Region	**Geographic Co-ordinates**	**Regional Characteristics**
Arid (North Africa)	15°-30°N, 11.5°W-30°E (Sahara desert)	Desert climate (sparse rainfall)
Semi-arid (northern and southern Africa)	12-15°N, 11.5°W-30°E (Northern Africa) 17° - 22°S, 17° – 30°E (Southern Africa)	Steppe climate (low rainfall)
Savanna (northern and southern Africa)	8°-12°N, 11.5°W-30°E (Western Africa) 6.5°-17°S, 14°-40°E (Southern Africa)	Hot dry season (moderate rainfall)
Tropical-wet	6.5°N - 6.5°S, 11.5°W - 30°E (between northern and southern savanna regions)	Wet climate (high, all-year rainfall)
South Atlantic Ocean	3.5°N-39.5S and 19.5°W-5.5°E	Oceanic climate

Table 2: Seasons in which the standard error of the PR, TMPI and TRMM_OS is less than 100% in each climatic region. The minimum seasonal mean (threshold) rainfall is also indicated. For the South Atlantic Ocean, TRMM_OS was used as reference.

Algorithm	**Climatic Region**	**Threshold** (Mean Seasonal Rainfall) [mm]	Applicable Seasons
PR	Arid (North)	-	-
	Semi-Arid (North)	42	JJA, SON
	Savanna (North)	46	MAM, JJA, SON
	Tropical-Wet	120	MAM, JJA, SON
	Semi-Arid (South)	30	DJF, MAM, SON
	Savanna (South)	75	DJF, MAM
	South Atlantic Ocean	21	DJF, MAM, JJA
TMPI & TRMM_OS	Arid (North)	8	MAM, SON
	Semi-Arid (North)	10	MAM, JJA, SON
	Savanna (North)	46	MAM, JJA, SON
	Tropical-Wet	72	DJF, MAM, JJA, SON
	Semi-Arid (South)	1	DJF, MAM, JJA, SON
	Savanna (South)	7	DJF, MAM, JJA, SON
	South Atlantic Ocean	21	DJF, MAM, JJA